2010 13th International IEEE
Annual Conference on Intelligent Transportation Systems
Madeira Island, Portugal, September 19-22, 2010

Following Vehicle Detection Based on Shift of Feature Plane Using Affine Transform

Shintaro ARAI, Osamu INOUE and Shinji OZAWA

***Abstract*— This paper proposes a novel vehicle detection system based on shift of a feature plane, which consisted of feature points on a front surface of vehicle, using in-vehicle camera for following vehicles' observation. We find that the feature plane of the vehicle's front surface shifts in accordance with the affine transform. We perform experiments and evaluate performances of our system. As results, we confirm that our system can locate and track the rear and side vehicles accurately and robustly.**

I. Introduction

In this paper, we develop a vehicle sensing technique using a camera as intelligent transport systems (ITS) applications. Our system targets at a warning system for saving collisions with approaching vehicles from behind and side The ITS applications using a camera is one of areas of active research by many researchers in the field of image processing [1]–[6]. The applications using the camera are grouped into two general categories depending on an installation location: One is an installation to roadway infrastructures (Roadside camera) [1]–[3]; Another is an installation to vehicles (In-vehicle camera) [4]–[6]. The former group aims at an analysis of a traffic flow and a detection of emergent events. The latter group aims at ensuring driving safety and drive assist. A common problem of these systems is that tracking of vehicle by image processing becomes difficult depending on illumination conditions due to a change of weather or period of time.

For solving this problem, a vehicle tracking system using feature points was proposed [1], [2]. It is easy to detect the feature points of the vehicle because the form of vehicle has many edge components such as corners of windows and a bumper, etc. In addition, the detection of the feature points does not depend on the weather and the time. However, the feature points are also detected from artifacts which appear in the background image such as guardrails and signs. Namely, the removal of unnecessary feature points is required for detecting the feature points of the vehicle. In the case of system using the roadside camera [1], [2], the system can treat as fixed objects since the camera is fixed in roadway infrastructures. Thus, the system using the roadside camera can remove unnecessary feature points derived from the background. On the other hand, in the case of the system using in-vehicle camera, the environment and the background are changed depending on the driving of the own vehicle. Thus, we consider that the system using in-vehicle camera is more difficult to remove unnecessary feature points than the system using the roadside camera.

This work was not supported by any organization

S. ARAI and S. OZAWA are with the ITS Laboratory, Faculty of Engineering, Aichi University of Technology, Gamagori Aichi 443-0047, JAPAN arai-its@aut.ac.jp, ozawa@aut.ac.jp

O. INOUE is with the Graduate School of Science and Technology, Keio University, Yokohama Kanagawa 223-8522, JAPAN

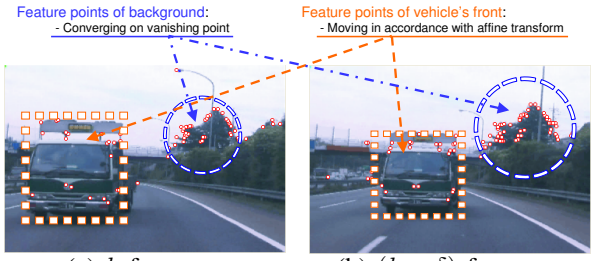

(a) k frame (b) $(k-\delta)$ frame

Fig. 1. Behavior of feature points on vehicle's front surface.

For removing unnecessary feature points, we consider the vehicle front surface as planar and assume it follows an affine transform. We find that this affine transform assumption is valid, and the optical flow of the plane is used to determine whether it belongs to the background or to a following vehicle. Namely, our system can differentiate the front face of following vehicle and the background.

Based on above characteristics, we propose a novel vehicle detection method using the affine transform. Moreover, for increasing the robustness of the vehicle tracking, we also show a vehicle position estimation method. We perform experiments and evaluate the performance of our system.

II. Concept of Proposed Method

In this section, we describe a concept of the proposed vehicle detection system. Our system uses Lucas-Kanade method (LK method) which is well-known as a typical feature point's detection algorithm [7]. As described in Sect. 1, the removal of unnecessary feature points is required for detecting the feature points of the vehicle. For removing unnecessary feature points, we focus on a relationship between feature points and the affine transform.

Figure 1 shows an image detected feature points from a still image which captured the approaching vehicle using the in-vehicle rear camera. Figures 1(a) and (b) indicate the image of k frame and $(k-\delta)$ frame, respectively, where δ denotes the number of time delay. We focus on the feature points of the front surface. Here, we assume the front surface of vehicle of Figs. 1(a) and (b) as the planar surface. Compared with two planar surfaces, the observing vehicle approaches the rear camera without almost changing the form of the plane between k frame and $(k-\delta)$ frame. From this characteristic, we consider that the front surface of vehicle shifts in accordance with the affine transform. Moreover, since the own vehicle drives toward the direction of forward movement, the feature points of motionless objects and the background back away from the camera. In other words, motionless objects' feature points converge on a vanishing

978-1-4244-7658-9/10/$26.00 ©2010 IEEE

TABLE I

AVERAGE OF AFFINE PARAMETERS.

	Average of affine parameters			
	r_{11}	r_{12}	r_{21}	r_{22}
Front of vehicle	0.973	-0.019	0.013	0.829
Others	1.029	-0.116	0.026	0.838

TABLE II

VARIANCE OF AFFINE PARAMETERS.

	Variance of affine parameters			
	r_{11}	r_{12}	r_{21}	r_{22}
Front of vehicle	0.019	0.005	0.008	0.016
Others	2.492	10.921	1.535	7.921

point. Therefore, it can be said that the behavior of feature points is different between the observing vehicle and others.

Next, we describe the affine transform of the front of vehicle. The affine transform is performed by Eq. (1).

$$\begin{pmatrix} x_k \\ y_k \\ 1 \end{pmatrix} = \begin{pmatrix} r_{11} & r_{12} & r_{13} \\ r_{21} & r_{22} & r_{23} \\ 0 & 0 & 1 \end{pmatrix} \begin{pmatrix} x_{k-\delta} \\ y_{k-\delta} \\ 1 \end{pmatrix} \quad (1)$$

where x_k and y_k denote the coordinate of the feature point in k frame, r_{11}–r_{23} denote the affine parameters. Also, the affine parameters are expressed as an affine matrix $\mathbf{P}$ shown in Eq. (2).

$$\mathbf{P} = \begin{pmatrix} r_{11} & r_{12} & r_{13} \\ r_{21} & r_{22} & r_{23} \\ 0 & 0 & 1 \end{pmatrix} \quad (2)$$

where r_{11} and r_{22} denote the scale, r_{12} and r_{21} denote the rotation, r_{13} and r_{23} denote the translation component.

Here, we assume that the front surface of vehicle shifts in accordance with the affine transform. In this case, we can regard that the observing vehicle's front surface changes the scale a little and hardly rotate. When the affine matrix $\mathbf{P}$ is calculated from feature points of the observing vehicle's front surface, each average of r_{21} and r_{22} approaches zero, and each average of r_{11} and r_{22} approaches one, as shown in Tab. I. In addition, each variance of r_{11}, r_{12}, r_{21} and r_{22} becomes small value, as shown in Tab. II. Therefore, we consider that it can be decided whether the observing vehicle's feature points or not by performing a threshold processing of the affine matrix. Based on this concept, we propose a novel vehicle detection method in the next section.

III. PROPOSED VEHICLE DETECTION SYSTEM

A. Experimental Vehicle

In this study, the proposed system uses three cameras (Rear, Left and Right sides) for covering all blind area. We set up the cameras to the sedan car, as shown in Fig. 2. For setting the position of the cameras, we referred available vehicles having the driving support system using the camera. Also, a view angle of the rear and side camera is 110° and 70°, respectively. Figure 3 shows the input images captured from each camera.

B. Flow of Proposed System

Figure 4 shows a flow chart of the proposed vehicle detection system. Here, we describe the brief flow of our system. First, our system restricts a processing region of the input image. Second, using LK method, the feature

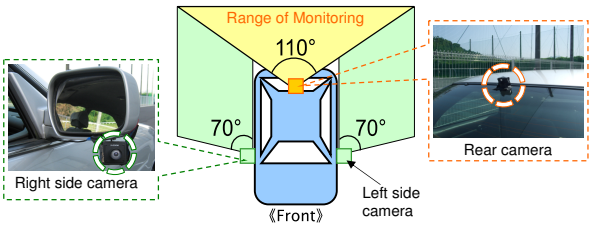

Fig. 2. Experimental vehicle with in-vehicle cameras.

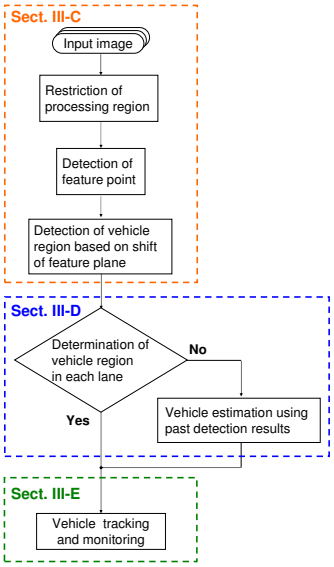

Fig. 4. Flow of proposed vehicle detection.

points are detected from the input image. Third, using the affine parameters, the system detects the vehicle's feature points from the remaining unnecessary feature points, i.e. the detection of the front surface of the vehicle. Fourth, for preventing the oversight of the vehicle, the vehicle position estimation method is performed when the oversight of the vehicle occurs in the previous process. Finally, the system performs the tracking and monitoring of the detected vehicles.

As shown in Fig. 4, the brief flow of the system using the rear and side cameras has a commonality although each view angle of cameras and the captured images are different between the side and the rear. First, we describe common processes between the side and the rear. After that, we explain some different processes between the side and the rear.

C. Processes of Vehicle Detection

1) Restriction of Processing Region: Our system detects the feature points from the input image for detection of approaching vehicles. However, there are some regions which vehicles do not pass in the image. Therefore, we restrict the processing region of the input image as the preprocessing of the detection of feature points. In this study, the region's restriction method is different between the side and the rear. We explain each operation of the region's restriction method in Sect. III-F.1 and III-G.1.

2) Detection of Vehicle's Feature Points Using Affine Parameters: First, our system detects feature points and connects corresponding points between k frame and $(k-\delta)$

(a) Right (b) Rear (c) Left

Fig. 3. Images by in-vehicle camera.

frame. We decide δ in the preliminary experiment since δ influences the calculation of the affine parameters. As result of the preliminary experiment, we find that a suitable value of δ in our environment is five. Thus, we set $\delta = 5$ in this paper.

Second, our system calculates the affine parameters between three arbitrary corresponding points. Here, we define the total number of the detected feature points in k frame as M. In addition, we indicate the m-th feature point as $p_m^k = (x_m^k, y_m^k)$. Moreover, we define the set of the feature points at k and $(k-\delta)$ as $\mathbf{F}^k$ and $\mathbf{F}^{k-\delta}$, respectively. Thus, $\mathbf{F}^k$ and $\mathbf{F}^{k-\delta}$ can be expressed as following equations.

$$\mathbf{F}^k = \{p_0^k, p_1^k, \cdots, p_m^k \cdots, p_{M-1}^k\} \quad (3)$$

$$\mathbf{F}^{k-\delta} = \{p_0^{k-\delta}, p_1^{k-\delta}, \cdots, p_m^{k-\delta} \cdots, p_{M-1}^{k-\delta}\} \quad (4)$$

Third, we choose 3-combinations of points from $\mathbf{F}^k$ and $\mathbf{F}^{k-\delta}$, and calculate the affine matrix $\mathbf{P}_j$. This process is performed using all combinations ($j = 0, 1, \cdots, {}_MC_3 - 1$). As described in Sect. II, the average and the variance of calculated affine parameters are different between the vehicle's front and others. We perform a preliminary experiment in advance and decide the threshold of the average and the variance based on Tabs. I and II. Therefore, our system decides whether the observing vehicle's feature points or not by performing a threshold processing of the affine matrix.

Fourth, we calculate the difference D_j between the remained points of $\mathbf{F}^k$ and its corresponding points of $\mathbf{F}^{k-\delta}$ multiplied by $\mathbf{P}_j$ (i.e. $\mathbf{P}_j\mathbf{F}^{k-\delta}$) as follows.

$$D_j = |\mathbf{F}^k - \mathbf{P}_j\mathbf{F}^{k-\delta}| \quad (5)$$

If the front of vehicle approaches in accordance with the affine transform, $\mathbf{F}^k$ and $\mathbf{P}_j\mathbf{F}^{k-\delta}$ become almost the same value, namely, D_j approaches zero. After calculating D_j in all combinations, our system selects the smallest D_j. In addition, our system decides $\mathbf{P}_j$ of the smallest D_j as $\mathbf{P}_{best}$.

Finally, our system decides p_m^k, which satisfies the following equation using $\mathbf{P}_{best}$, as the observing vehicle's feature points.

$$\theta \geq |\mathbf{P}_{best} \cdot p_m^{k-\delta} - p_m^k| \quad (6)$$

Here, θ of Eq. (6) is decided in the advance preliminary experiment based on Tabs I and II

3) Determination of Vehicle's Front Surface: Based on the previous process's results, our system determines whether the observing vehicle's front surface or not. We observe size differences of the rectangle formed by feature points over f_{th} frames, and decide the rectangle as the observing vehicle's front surface if the size differences between f_{th} frames are flat. For performing a threshold processing of the size differences, we decide f_{th} in the preliminary experiment. As result of the preliminary experiment, we find that a suitable value of δ in our environment is five. Thus, we set $f_{th} = 5$ in this paper.

D. Vehicle Position Estimation Method Using Linear Extrapolation Algorithm

Although our system detects the observing vehicle's front surface in the previous process, the oversight of the vehicle might occur due to a sudden change of a brightness of an image depending on the driving environments. For reducing the oversight of the vehicle, we perform the vehicle position estimation method using a linear extrapolation algorithm.

Here, we assume the frame number detected the vehicle's front as fs_k, the relative distance d_k between the own vehicle and the detected vehicle, and the central x-coordinate Xc_k of the detected vehicle, as shown in Fig. 5. Based on d_k and Xc_k, we calculate the estimated relative distance d'_k and the estimated central x-coordinate Xc'_k for the vehicle position estimation. For example, when the oversight of the vehicle occurs, the slope a_d, the intercept b_d of the approximate lines of d_k and d'_k are calculated as follows.

$$a_d = \frac{n\sum_{k=1}^{n} fs_k d_k - \sum_{k=1}^{n} fs_k \sum_{k=1}^{n} d_k}{n\sum_{k=1}^{n} fs_k^2 - \left(\sum_{k=1}^{n} fs_k\right)^2} \quad (7)$$

$$b_d = \frac{\sum_{k=1}^{n} fs_k^2 \sum_{k=1}^{n} d_k - \sum_{k=1}^{n} fs_k d_k \sum_{k=1}^{n} fs_k}{n\sum_{k=1}^{n} fs_k^2 - \left(\sum_{k=1}^{n} fs_k\right)^2} \quad (8)$$

$$d'_k = a_d \cdot fs'_k + b_d \quad (9)$$

where n denotes the number of the frame succeeded in the vehicle detection using affine parameters. In the same way, $X'c_k$ can be calculated.

Here, the range of n is $(n_{min} \leq n \leq n_{max})$. In this study, we set $n_{min} = 5$ based on the determination of $f_{th} = 5$. On the other hands, n_{max} is different between the side and the rear. We explain each n_{max} in Sect. III-F.2 and III-G.2.

Using the vehicle position estimation, it is possible to continue to the observation of the vehicle's position even if the oversight of the vehicle occurs.

E. Tracking and Monitoring of Front of Vehicle

Using the area recognized as the front of the vehicle in the previous process, we perform the tracking and monitoring of

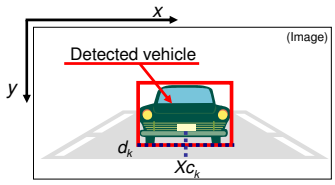

Fig. 5. d_k and Xc_k for Estimation.

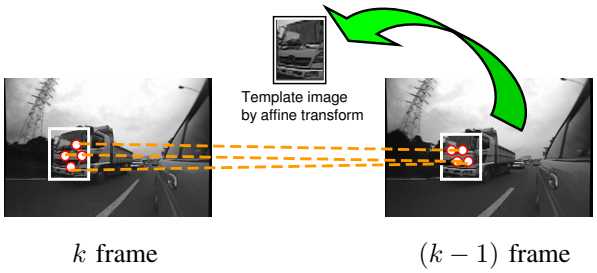

Fig. 7. Update of template of side vehicle by affine transform.

the detected vehicles. For the tracking, we use the variable template matching based on the normalized correlation. The template is updated using the front of the detected vehicle every frame. In this study, the updating method of the template is different between the side and the rear. We explain each updating method in Sect. III-F.3 and III-G.3.

F. Side Vehicle Detection

1) Restriction of Processing Region in Side Camera: For restriction of the processing region, the system in the side camera removes unnecessary feature points detected from the upper part of the image, the neighborhood of the lane and the own vehicle, based on the shooting angle of the camera and the lane information known in advance. We show the instance of the processing region's restriction and the vehicle detection result in Fig. 6.

2) Determine of n_{max} in Side Camera: We consider that it is highly possible that the side vehicles move continuously in the side image since almost side vehicles approach or leave from the own vehicle. In other words, we can assume that the observation time of the side vehicle is short in the image. Therefore, we set $n_{max} = 30$ (1 sec).

3) Updating Method of Template in Side Camera: When the vehicle is far from the own vehicle, we can update the template since the side camera can capture front surface of the detected vehicle. However, according to the approach of the vehicle, we can not simply use the detected vehicle's front since the camera captures the side surface of the vehicle.

For updating the template in the side, we also apply the affine transform. Figure 7 shows the example of the updating of the template using the affine transform. First, we calculate the affine parameters $\mathbf{P_t}$ using corresponding feature points between k frame and $(k-1)$ frame. Next, the vehicle's front in $(k-1)$ frame is multiplied by the calculated parameters $\mathbf{P_t}$. The vehicle's front multiplied by $\mathbf{P_t}$ in $(k-1)$ frame becomes the updated template for k frame. Therefore, we can perform the stable tracking and monitoring in the side camera.

G. Rear Vehicle Detection

1) Restriction of Processing Region in Rear Camera: Since the rear camera captures multiple lanes, it is highly possible that many observing vehicles are captured. In addition, the number of the feature points detected from the rear image is larger than that of the side image because there are many artifacts and objects in the rear image. Thus, the rear vehicle detection requires substantial time for detecting the vehicle if the same algorithm of the side is applied.

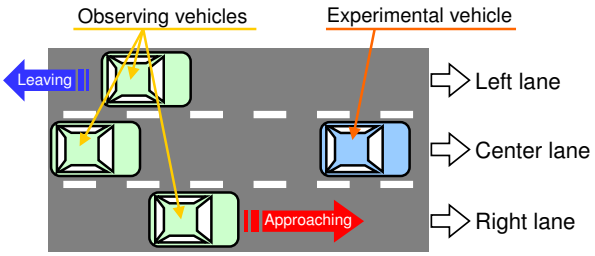

Fig. 9. Experimentation environment.

To solve this problem, we decide candidate regions of the vehicles using other image processing method as processing regions. In this study, we detect edge components of the rear image [4], [5] and decide the candidate regions. Here, we explain this operation using Fig. 8. First, we detect the horizontal edge component of the input image (Fig. 8(a)) from the bottom of the image toward the vanishing point. In addition, the region containing strong edge components is decided as the vehicle's search range in the horizontal direction, as shown in Fig. 8(b). Next, we detect the vertical edge component of the image. Since the strong vertical edge component is detected from the boundary between the vehicle and the background, the vehicles and the background can be divided by calculating the strength of the vertical edge component, as shown in Fig. 8(c). Finally, we find the strength horizontal edge area within the divided areas in the vertical direction, and decide these areas as the candidate regions of the vehicles, as shown in Fig. 8(d).

2) Determine of n_{max} in Rear Camera: In the rear vehicle position estimations, we set $n_{max} = 150$. The reason for this is that the difference of the capture environment between the rear and the side. Since the rear camera captures the many objects except vehicles compared with the side camera, the percentage of the change of the rear image's brightness is higher than that of the side. Thus, the number of the oversight frame of the vehicle might increase transiently depending on the background. To solve this problem, we increase the range of the observation of vehicle's detected results.

3) Updating Method of Template in Rear Camera: In the case of the rear camera, it is easy to update the template since the front of the vehicle approaches the camera without almost changing the form, as shown in Fig. 1. Thus, we can perform the stable tracking and monitoring in the rear camera.

IV. Experiments

A. Experimental setup and Evaluation method

To evaluate the accuracy and the computation cost of the proposed vehicle detection system, we perform a field experiment using the experimental vehicle of Fig. 2. As an experimentation environment, we choose a three-lane expressway. The experimental vehicle drives at 80km/h and captures the image sequences using three cameras. Moreover, we assume that the own vehicle drives on the center

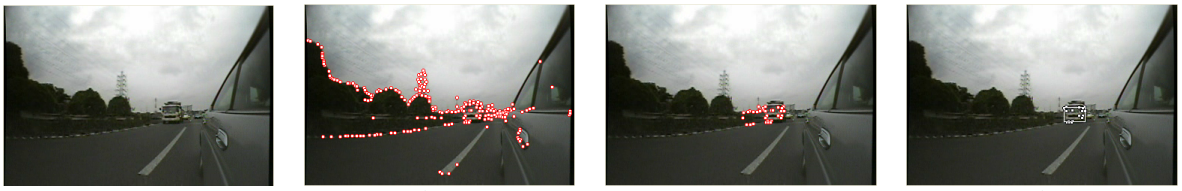

(a) (b) (c) (d)

Fig. 6. Detection of approaching side vehicle: (a) Input image, (b) Image with feature points without restriction of processing region, (c) Image with feature points with restriction of processing region, (d) Detected front vehicle region.

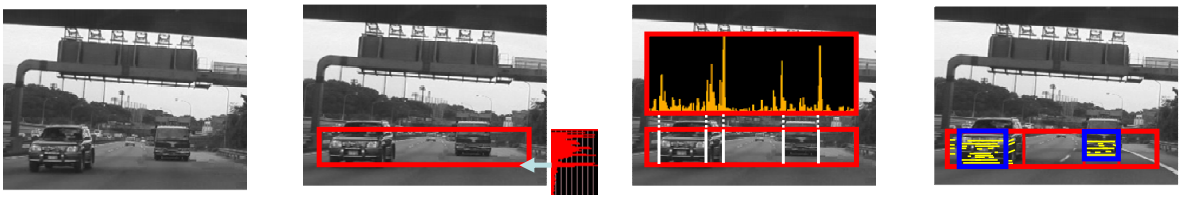

(a) (b) (c) (d)

Fig. 8. Detection of candidate vehicle region using edge component: (a) Input image, (b) Vehicle search range by horizontal edge, (c) Partition based on vertical edge, (d) Candidate vehicle region.

lane in three lanes and does not change the lane because the approaching and leaving vehicles are captured by side cameras. Tables III and IV show the experimental setup and the specification of desktop computer using this study, respectively. The image sequences are recorded in the hard disk. The vehicle detection experiment is performed by image processing of the computer.

In the image processing, the side camera observes the vehicles in each side lane only. On the other hand, the rear camera observes the vehicles in three lanes because the rear camera can capture the images in three lanes. All image sequences are experimental objects for the vehicle detection. Our system is designed that the front of the vehicle is enclosed by the rectangle shown in Figs. 6(d) when the vehicle is detected,

In this experiment, we use a two-by-two table shown in Tab. V and classify the detected results into four groups: True Positive (*TP*), False Negative (*FN*), False Positive (*FP*) and True Negative (*TN*). Based on the four groups, we calculate three evaluation values: "Precision (*P*)", "Recall (*R*)" and "Efficiency (*E*)". The three evaluation values are described by following equations.

$$P = \frac{TP}{TP+FP} \tag{10}$$

$$R = \frac{TP}{TP+FN} \tag{11}$$

$$E = \frac{TP+TN}{TP+FN+FP+TN} \tag{12}$$

B. Experimental results and Discussions

Tables VI and VII show classification results of detected vehicles in the rear and the side vehicle detection system, respectively. In addition, Figs. 10 and 11 show evaluation values based on classification results. Here, evaluation values of Fig. 10 are calculated from the total of each classification result. For comparing the proposed method and the other vehicle detection method, we show the result of the method of Refs. [4], [5] in Fig. 10.

Moreover, we calculate a computation time per frame of the proposed vehicle detection method. As the results, we confirm that it takes 1.2sec/frame to operate our system.

TABLE III

EXPERIMENTAL SETUP.

Experimental Object	2500frames
Size of Image	360 × 240pixel
Frame Rate	30frame/sec

TABLE IV

SPECIFICATION OF DESKTOP COMPUTER.

CPU	Core i7 2.66GHz
Memory	3.0GB
OS	WindowsXP Pro(SP3)
Compiler	Visual C++ .NET 2003
Platform	VC++ and OpenCV

TABLE V

CLASSIFICATION OF RESULTS OF DETECTED VEHICLES.

		System	
		Detection	Not detection
Dose the vehicle exist in the image?	Yes	True Positive	False Negative
	No	False Positive	True Negative

TABLE VI

CLASSIFICATION RESULT OF DETECTED VEHICLE IN REAR CAMERA.

	TP	*FN*	*FP*	*TN*
Left Lane	1712	291	0	497
Center Lane	2049	418	0	33
Right Lane	1135	118	63	1184
Total	4896	827	63	1714

TABLE VII

CLASSIFICATION RESULT OF DETECTED VEHICLE IN SIDE CAMERAS.

	TP	*FN*	*FP*	*TN*
Left side	506	174	0	1820
Right side	793	19	443	1245

1) Discussion of Rear vehicle detection: As shown in Fig. 10, all evaluation values of our system are larger than the method of Refs. [4], [5]. Especially, *P* is significantly-large and is up by more than 10% from the method of Refs. [4], [5]. Therefore, it can be said that our system achieves the low false detection, and can perform the stable vehicle detection.

However, it can be observed that *FN* is larger than *FP* in the rear vehicle detection, as shown in Tab. VI. Especially,

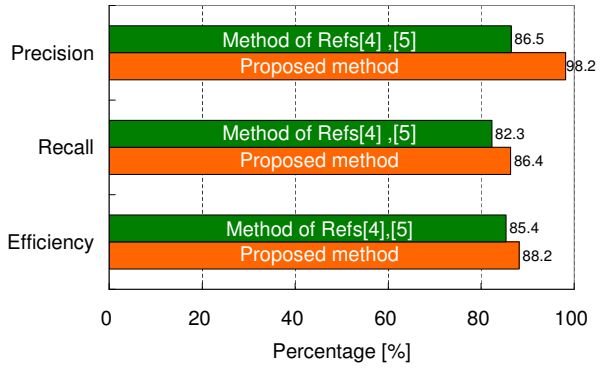

Fig. 10. Accuracy rate of following vehicle detection using rear camera.

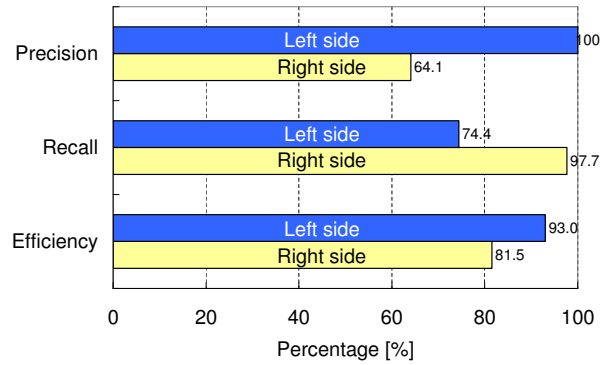

Fig. 11. Accuracy rate of side vehicle detections using side cameras.

FN of the center lane is largest in all lanes. We consider that the reason for this is the influence of the relative velocity between the experimental vehicle and the observing vehicle. When the experimental and observing vehicles drive in the identical lane, the relative velocity between two vehicles approaches zero. In addition, when the observing vehicle keeps a safe distance between two vehicles, the number of the feature points of the vehicle's front decreases since the image resolution of the observing vehicle becomes low. For reducing *FN*, we consider that the proposed rear vehicle detection requires cooperating with static-image processing.

2) Discussion of Side vehicle detection: As shown in Fig. 11, in the case of the left side, *P* is very high, i.e. the false detection is low. However, *R* is low since a large number of *FN* is observed as shown in Tab. VII. In other words, the oversight of the vehicle occurs mostly in the left side. On the other hand, in the case of the right side, *R* is very high, i.e. the oversight of the vehicle is low. However, *P* is low since a large number of *FP* is observed. Namely, the result of the right side shows the opposite result of the left side.

We consider that the reason for this is difference of the vehicle's influence between the left and right lanes In general rule of Japanese road, three lanes are classified into the first driving lane (Left lane), second driving lane (Center lane) and the fast lane (Right lane). In this study, the experimental vehicle drives on the center lane, i.e. the second driving lane. In the left side lane, we observe many scenes that the experimental vehicle overtakes the observing vehicle. On the other hands, we observe many scenes that the observing vehicle of the right side lane overtakes the experimental vehicle.

Let us discuss the results of the left side. When the own vehicle overtakes the observing vehicle, the side camera captures the side surface of the observing vehicle at the beginning, and gradually captures the front surface of the observing vehicle. Since our system observes the change of the affine parameters of the vehicle's front, the delay of the observing vehicle's detection occurs. However, once the observing vehicle's front surface is detected, the propose method can perform the stable vehicle tracking

In a similar way, we discuss the results of the right side. When the observing vehicle overtakes the own vehicle from a long distance, the proposed method can early detect the observing vehicle since the front surface of the observing vehicle gradually zooms in the side camera. Therefore, the oversight of the vehicle becomes low since *FN* decreases. However, it is also confirmed that the number of *FP* influences the calculation of *P*. We consider that the reason for this is the influence of the estimated error by the vehicle position estimation method. In the results of the right side, *FP* often occurs in the successive scene appearing the roadside surface with the same texture. In this case, the result of *FP* is used for the calculation of the estimation as correctly detected vehicle. Thus, the extra *FP* is observed due to the estimated error. Therefore, the reduction of the estimation error is important matter of future work.

3) Computation cost of Proposed system: Finally, we summarize the computation cost per frame of the proposed vehicle detection method. As described above, it takes 1.2sec/frame to operate our system. Since the frame rate of the camera is 30frame/sec in this study, our system currently underperforms the real-time process. Thus, by optimizing some parameters without decreasing the detection characteristics, a reducing of the computation cost is also important matter of future work.

V. Conclusions

In this paper, we have proposed the novel vehicle detection method using the affine transform and the movement of the feature plane with in-vehicle camera. As results of the experiment, we have confirmed that the rear vehicle detection achieves the low false detection, and can perform the stable vehicle detection. In addition, we have observed that the difference of the relative velocity influences the characteristics.

References

[1] M. Ambai and S. Ozawa, "Traffic Monitoring System for Measuring Number of Vehicles in Various Environments," *Proc. FCV'05*, pp. 160-165, Jan. 2005.
[2] M. Ambai and S. Ozawa, "Occlusion Robust Tracking Using Constrained Graph Cuts," *IEICE Trans. Fundamentals*, vol. J90-A, no. 12, pp. 948-959, Dec. 2007. (in Japanese)
[3] F. Lamosa, Z. Hu and K. Uchimura, "Vehicle Detection Using Probability Fusion Maps Generated by Multi-camera Systems," *J. Information Processing*, vol. 17 pp, 1-13, Jan. 2009.
[4] T. Yasumasu and S. Ozawa, "Observation of Rear of Vehicle Using a Camera in-Vehicle, 9th World Congress on ITS, 2002.
[5] T. Yasumasu and S. Ozawa, "Detection of Dangerous Vehicles from Rear Scene," *IEEJ Trans. Electronics, Information and Systems*, Vol. 125, No. 4, pp. 570-575, Apr. 2005. (in Japanese)
[6] C. Yang, H. Hongo and S. Tanimoto, "A New Approach for In-Vehicle Camera Obstacle Detection by Ground Movement Compensation," *Proc. ITSC'08*, pp. 151-156, Oct. 2008.
[7] J. Shi and C. Tomasi, "Good features to track," *Proc. CVPR*, pp. 593-600, June 1994.